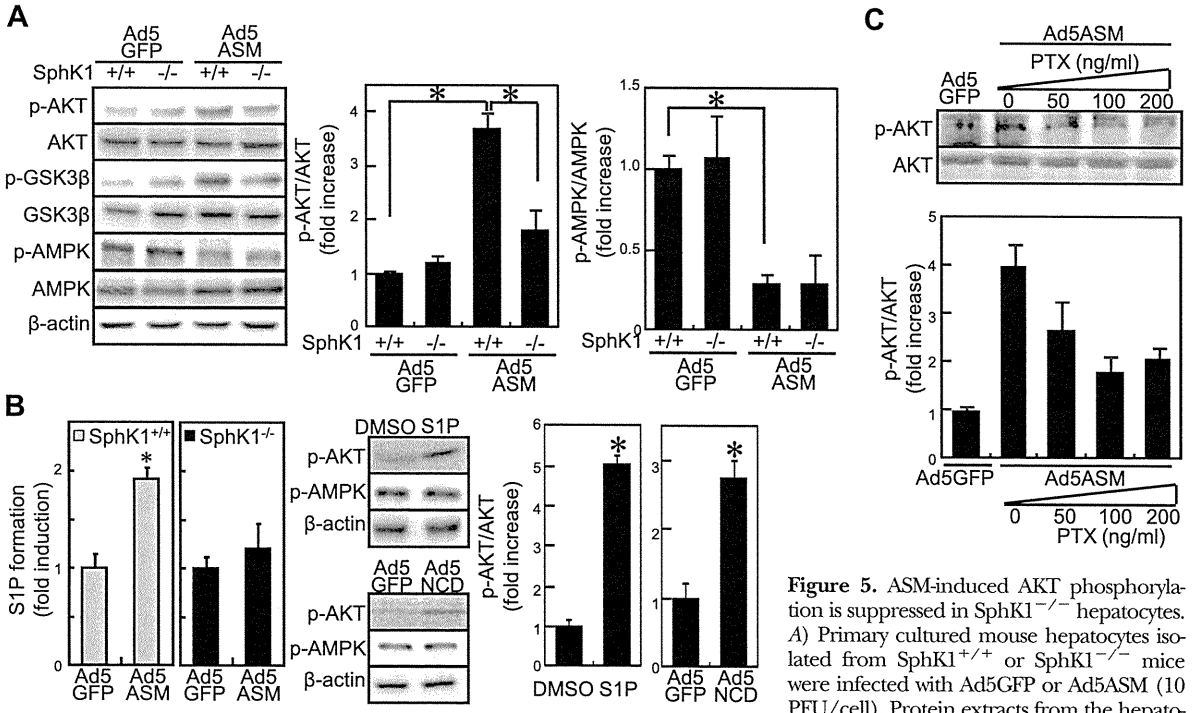

Figure 5. ASM-induced AKT phosphorylation is suppressed in SphK1$^{-/-}$ hepatocytes. *A*) Primary cultured mouse hepatocytes isolated from SphK1$^{+/+}$ or SphK1$^{-/-}$ mice were infected with Ad5GFP or Ad5ASM (10 PFU/cell). Protein extracts from the hepatocytes were subjected to immunoblot for phosphorylated (p)-AKT, AKT, p-GSK3β, GSK3β, p-AMPK, AMPK, and β-actin. *B*) [^{3}H]Serine-labeled hepatocytes from SphK1$^{+/+}$ or SphK1$^{-/-}$ mice were infected with Ad5GFP or Ad5ASM. Radiolabeled S1P was measured (left panels). Primary cultured rat hepatocytes were treated with or without S1P (1 μM) for 8 h (middle top panel). Primary cultured rat hepatocytes were infected with Ad5GFP or adenovirus expressing human neutral ceramidase (Ad5NCD) (middle bottom panel). Protein extracts from the hepatocytes were subjected to immunoblot for p-AKT, p-AMPK, and β-actin. *C*) Primary cultured rat hepatocytes were infected with Ad5GFP or Ad5ASM (10 PFU/cell), and incubated for 2 h. Then, cells were treated with or without the indicated concentration of PTX for 24 h. Top panel: protein extracts from hepatocytes were subjected to immunoblot for p-AKT and AKT. Relative densitometric intensity of p-AKT and p-AMPK was determined for each protein band of the sample and normalized to AKT and AMPK, respectively (*A*, *B*, right panels; *C*, bottom panel). Results shown are representative of ≥3 independent experiments. Data are means ± SD from ≥4 independent experiments. *$P < 0.05$.

cytes. In contrast, ASM deficiency inhibits glucose uptake, glycogen deposition, and lipid accumulation, resulting in glucose intolerance. In ASM$^{-/-}$ mice, similar levels of GSK3β phosphorylation were induced by food intake, whereas GLUT2 induction was reduced in comparison to the livers of ASM$^{+/+}$ mice (**Fig. 9*A***). Reduction of AMPK phosphorylation and induction of GLUT2 by high-dose glucose were inhibited in ASM$^{-/-}$ hepatocytes (Fig. 9*B*), whereas high-dose glucose did not affect AKT phosphorylation (data not shown). These results suggest that glu-

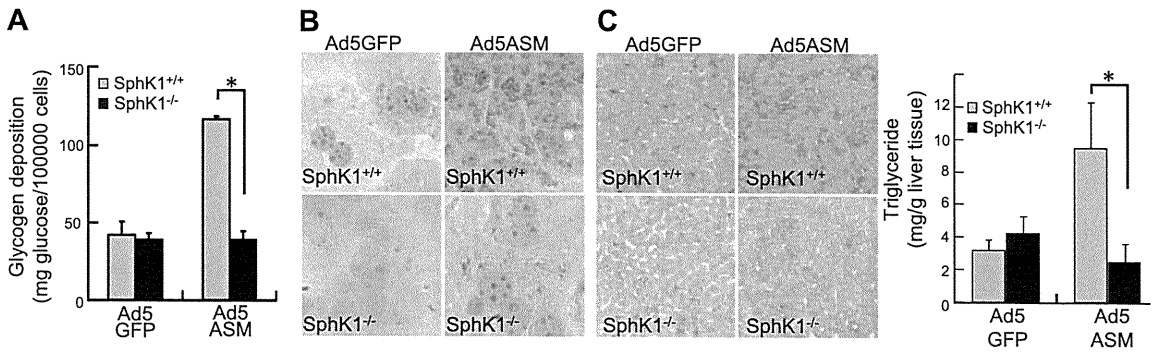

Figure 6. ASM-induced glycogen deposition and lipid accumulation are suppressed in SphK1$^{-/-}$ hepatocytes. *A*) Primary cultured hepatocytes isolated from SphK1$^{+/+}$ or SphK1$^{-/-}$ mice were infected with Ad5GFP or Ad5ASM. Glycogen content in hepatocytes was determined. *B*) Lipid droplets in SphK1$^{+/+}$or SphK1$^{-/-}$ hepatocytes infected with Ad5GFP or Ad5ASM were assessed by Oil Red O staining (original view ×800). *C*) SphK1$^{+/+}$ or SphK1$^{-/-}$ mice were infected with Ad5GFP or Ad5ASM, followed by assessment for hepatic lipid content by Oil Red O staining (left panel; original view ×200) and triglyceride measurement (right panel) in food-deprivation conditions at 7 d after the infection (original view ×200). Results shown are representative of ≥3 independent experiments. Data are means ± SD from ≥4 independent experiments. *$P < 0.05$.

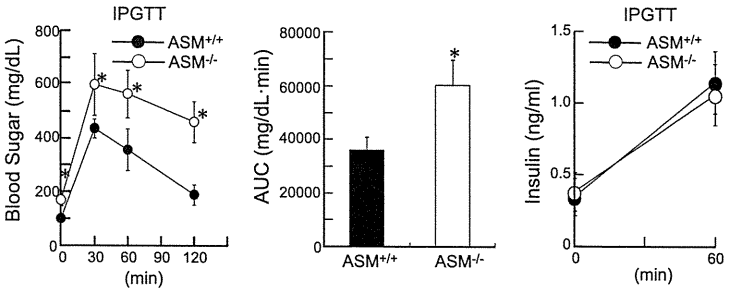

Figure 7. $ASM^{-/-}$ mice were glucose intolerant. *A*) $ASM^{+/+}$ and $ASM^{-/-}$ mice were deprived of food for 18 h, and IPGTT was performed by administering a glucose load of 2 mg/g body weight. Serial glucose (left panel) and insulin (right panel) were measured at the indicated time points. Blood glucose values for area under the curve (AUC) were calculated (middle panel). Results shown are representative of ≥3 independent experiments. Data are means ± SD from ≥4 independent experiments. $^*P < 0.05$.

cose intolerance in $ASM^{-/-}$ mice was due, at least in part, to insufficient reduction of AMPK activity and induction of GLUT2.

DISCUSSION

The present study addresses the contributions of ASM to glucose and lipid metabolism in the liver. The sphingomyelin/ceramide/S1P pathway is involved in glucose metabolism (6–9, 12–14, 21). Food intake reduced most sphingomyelin species in the mouse liver (Supplemental Table S2). Likewise, high-dose glucose reduced sphingomyelin species in primary cultured hepatocytes (Supplemental Table S2), suggesting that this pathway is related to glucose metabolism in hepatocytes. In our study using hepatocytes, ASM induced insulin-like effects such as glucose uptake, glycogen deposition, and lipid accumulation *via* S1P-mediated AKT activation. Ceramide attenuates insulin signaling, including AKT activation (14–16), thereby contributing to insulin resistance through multiple pathways (13, 15). In primary cultured hepatocytes, the effect of ASM introduction on ceramide level was smaller than that in sphingomyelin degradation, suggesting that the generated ceramide is further converted to S1P. Ceramide and S1P often exert opposing effects; thus, the balance between these two sphingolipids may be important for AKT activation. During ASM activation, the balance is inclined toward S1P, resulting in AKT activation. Indeed, ASM did not activate AKT in $SphK1^{-/-}$ hepatocytes, suggesting that ASM mediates insulin-like effects *via* S1P formation. S1P acts as a ligand for the S1PRs and also as an intracellular second messenger (31, 32). Among S1PRs, G_i-associated S1PR1 (33) is mainly expressed in the liver (34), and PTX pretreatment inhibited exogenous S1P-induced AKT phosphorylation in

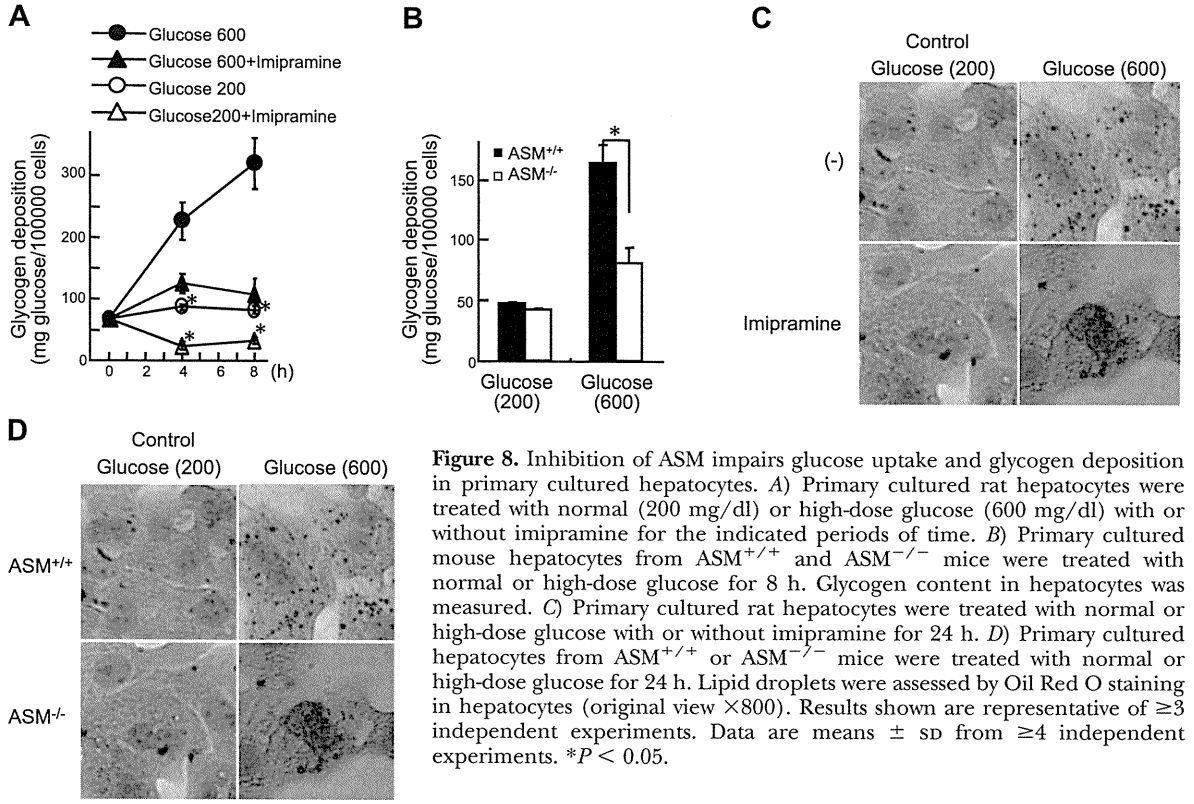

Figure 8. Inhibition of ASM impairs glucose uptake and glycogen deposition in primary cultured hepatocytes. *A*) Primary cultured rat hepatocytes were treated with normal (200 mg/dl) or high-dose glucose (600 mg/dl) with or without imipramine for the indicated periods of time. *B*) Primary cultured mouse hepatocytes from $ASM^{+/+}$ and $ASM^{-/-}$ mice were treated with normal or high-dose glucose for 8 h. Glycogen content in hepatocytes was measured. *C*) Primary cultured rat hepatocytes were treated with normal or high-dose glucose with or without imipramine for 24 h. *D*) Primary cultured hepatocytes from $ASM^{+/+}$ or $ASM^{-/-}$ mice were treated with normal or high-dose glucose for 24 h. Lipid droplets were assessed by Oil Red O staining in hepatocytes (original view ×800). Results shown are representative of ≥3 independent experiments. Data are means ± SD from ≥4 independent experiments. $^*P < 0.05$.

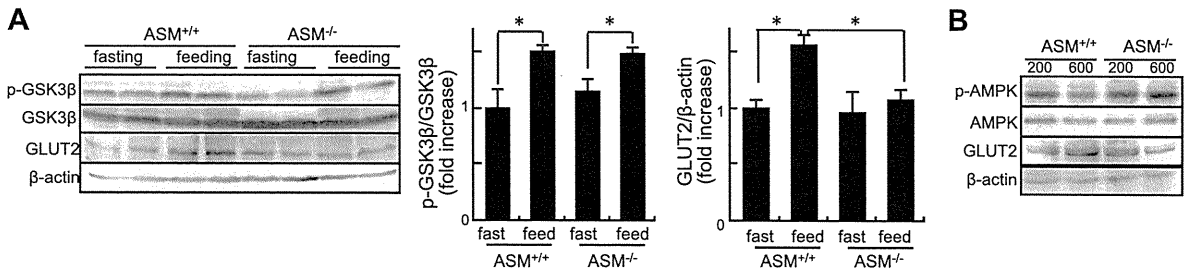

Figure 9. Inhibition of ASM suppresses GLUT2 induction. *A*) $ASM^{+/+}$ and $ASM^{-/-}$ mice were killed in both nonfeeding (fasting; 18 h food deprivation) and feeding conditions. Protein extracts from liver tissue were subjected to immunoblot for phosphorylated (p)-GSK3β, GSK3β, GLUT2, and β-actin (left panel). Relative densitometric intensity of p-GSK3β (middle panel) and GLUT2 (right panel) was determined for each protein band of the liver tissue sample and normalized to GSK3β and β-actin, respectively. *B*) Primary cultured hepatocytes from $ASM^{+/+}$ and $ASM^{-/-}$ mice were treated with normal (200 mg/dl) or high-dose glucose (600 mg/dl) for 8 h. Protein extracts from hepatocytes were subjected to immunoblot for p-AMPK, AMPK, GLUT2, and β-actin. Results shown are representative of ≥3 independent experiments. $*P < 0.05$.

primary cultured hepatocytes (data not shown), suggesting that S1P may activate AKT through predominantly S1PR1. PTX treatment partially inhibits ASM-induced AKT activation, suggesting that the generated S1P activates AKT at least partially *via* S1PRs and may also activate AKT through receptor-independent mechanisms.

In addition to AKT, AMPK also contributes to glucose metabolism. AMPK is a serine/threonine protein kinase that senses the immediate availability of cellular energy. Activated AMPK switches on catabolic pathways and switches off protein, carbohydrate, and lipid biosynthesis (anabolic pathways; ref. 35). Activation of AMPK in the liver reduces glycogen synthesis and lipogenesis as well as expression of GLUT2 (3). Activation of AMPK by 5-amino-4-imidazolecarboxamide riboside diminishes GLUT2 expression in primary cultured hepatocytes (36). Indeed, DN-AMPK increased glycogen deposition and lipid accumulation in primary hepatocytes and HepG2 cells (data not shown and ref. 37). Thus, in addition to increased AKT activation, reduced AMPK activation may be associated with another anabolic effect of ASM. Ceramide decreases (38) but S1P increases (39) AMPK phosphorylation in endothelial cells. In our study, ASM-induced AMPK inhibition in hepatocytes was independent of S1P. Thus, the decrease in AMPK activity may be due to ceramide processed by ASM.

Ad5ASM-infected mice showed improved glucose tolerance. Because adenovirus preferentially infects hepatocytes, the decrease in blood glucose was due to a variation of hepatic glucose metabolism, although sphingolipids have roles in glucose metabolism in muscle (40) and adipocytes (6–8). The ASM-induced decrease in blood glucose may be attributed to increased uptake of hepatic glucose rather than decreased production, because introduction of ASM did not affect the activity of adenylate cyclase, the glucagon target enzyme, in primary cultured rat hepatocytes (data not shown). The effects of ASM on hepatocytes are comparable to those of insulin. However, the introduction of hepatic ASM improved hyperglycemia in *db/db* mice with type 2 diabetes without increasing insulin levels (data not shown), indicating that ASM may reduce blood glucose regardless of the presence of insulin resistance. Instead of decreasing blood glucose, ASM increased hepatic triglyceride content, suggesting that ASM stimulates lipogenesis, in which transported glucose is converted to triacylglycerol (41). The effects of exogenous ASM in the liver are similar to the effects of deletion of hepatic phosphatase and tension homolog on chromosome 10 (PTEN), which is a negative regulator of AKT. Deletion of PTEN in the liver results in hyperphosphorylation of hepatic AKT and improves glucose tolerance but induces fatty liver in mice (42).

$ASM^{-/-}$ mice are glucose intolerant. The abnormality is not due to inactivation of the AKT/GSK3β pathway but is due, in part, to insufficient reduction of AMPK activity and induction of GLUT2. In addition, crosstalk may occur between ASM and various signaling pathways, including those of glucose and lipid metabolism, because ASM regulates sphingolipids in lipid raft microdomains that function as platforms for signal transduction and protein sorting (18). For example, disruption of lipid raft microdomains or chronic ethanol exposure inhibits localization of TC10 to lipid rafts,

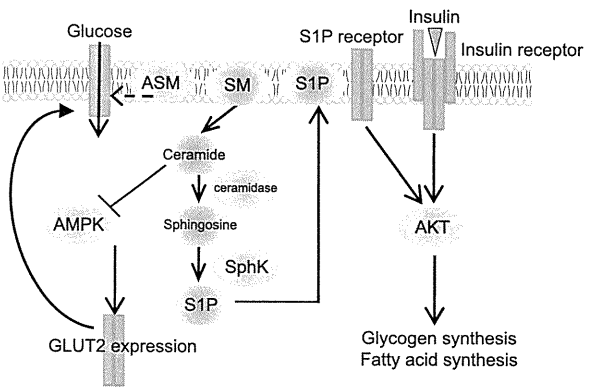

Figure 10. Hypothetical signals induced by ASM. Acid sphingomyelinase regulates glucose and lipid metabolism through AKT activation and AMPK suppression in hepatocytes. AKT activation is induced through S1P formation. AMPK suppression increases GLUT2 expression.

which induces GLUT4 translocation and glucose intake without affecting phosphatidylinositol-3 kinase/AKT signaling in adipocytes (43, 44). Pretreatment with imipramine inhibited high-dose glucose-induced lipid accumulation in rat hepatocytes, as did the knockout of ASM in mouse hepatocytes. As reported previously, the ASM inhibitor desipramine attenuates triglyceride increase by high-dose palmitic acid treatment in HepG2 cells (9). Moreover, a high-fat, high-cholesterol diet does not induce hepatic triacylglyceride accumulation in $ASM^{-/-}$ mice under LDL receptor-deficient conditions (9). These observations further support the role of ASM as a regulator of triglyceride synthesis in addition to glucose uptake. Further studies will determine the precise mechanism underlying the anabolic effects of ASM and its activation and ceramide/S1P regulation (45). The hypothetical roles of ASM are schematically summarized in **Fig. 10**.

In conclusion, overexpression of ASM in the liver improves glucose tolerance in both wild-type and diabetic *db/db* mice. ASM stimulates glucose uptake, glycogen deposition, and lipid accumulation in hepatocytes *via* AKT and GSK3β phosphorylation, which requires S1P formation. In addition, ASM decreases AMPK phosphorylation through ceramides, leading to GLUT2 up-regulation. Indeed, inactivation of ASM produces glucose intolerance in hepatocytes. Targeting ASM may become a new therapeutic strategy in type 2 diabetes. FJ

The authors thank Dr. Jacek Bielawski (Medical University of South Carolina, Charleston, SC, USA) for sphingolipid measurement, Dr. Yoko Sugiyama (Gifu University Graduate School of Medicine, Gifu, Japan) for measurement of adenylate cyclase activity, and Dr. Kenneth Walsh (Boston University, Boston, MA, USA) for adenoviruses encoding CA-AMPK and DN-AMPK. This work was supported by grants from Mitsubishi Pharma Research Foundation and the Ministry of Education, Culture, Sports, Science, and Technology of Japan (19790478 and 21790657 to Y.O. and 21390179 to M.S.).

REFERENCES

1. Thorens, B., Sarkar, H. K., Kaback, H. R., and Lodish, H. F. (1988) Cloning and functional expression in bacteria of a novel glucose transporter present in liver, intestine, kidney, and β-pancreatic islet cells. *Cell* **55,** 281–290
2. Rencurel, F., Waeber, G., Antoine, B., Rocchiccioli, F., Maulard, P., Girard, J., and Leturque, A. (1996) Requirement of glucose metabolism for regulation of glucose transporter type 2 (GLUT2) gene expression in liver. *Biochem. J.* **314**(Pt. 3), 903–909
3. Foretz, M., Ancellin, N., Andreelli, F., Saintillan, Y., Grondin, P., Kahn, A., Thorens, B., Vaulont, S., and Viollet, B. (2005) Short-term overexpression of a constitutively active form of AMP-activated protein kinase in the liver leads to mild hypoglycemia and fatty liver. *Diabetes* **54,** 1331–1339
4. Smith, E. L., and Schuchman, E. H. (2008) The unexpected role of acid sphingomyelinase in cell death and the pathophysiology of common diseases. *FASEB J.* **22,** 3419–3431
5. Gorska, M., Baranczuk, E., and Dobrzyn, A. (2003) Secretory Zn2+-dependent sphingomyelinase activity in the serum of patients with type 2 diabetes is elevated. *Horm. Metab. Res.* **35,** 506–507
6. Liu, P., Leffler, B. J., Weeks, L. K., Chen, G., Bouchard, C. M., Strawbridge, A. B., and Elmendorf, J. S. (2004) Sphingomyelinase activates GLUT4 translocation via a cholesterol-dependent mechanism. *Am. J. Physiol. Cell Physiol.* **286,** C317–C329
7. David, T. S., Ortiz, P. A., Smith, T. R., and Turinsky, J. (1998) Sphingomyelinase has an insulin-like effect on glucose transporter translocation in adipocytes. *Am. J. Physiol.* **274,** R1446–1453
8. Al-Makdissy, N., Younsi, M., Pierre, S., Ziegler, O., and Donner, M. (2003) Sphingomyelin/cholesterol ratio: an important determinant of glucose transport mediated by GLUT-1 in 3T3–L1 preadipocytes. *Cell. Signal.* **15,** 1019–1030
9. Deevska, G. M., Rozenova, K. A., Giltiay, N. V., Chambers, M. A., White, J., Boyanovsky, B. B., Wei, J., Daugherty, A., Smart, E. J., Reid, M. B., Merrill, A. H., Jr., and Nikolova-Karakashian, M. (2009) Acid sphingomyelinase deficiency prevents diet-induced hepatic triacylglycerol accumulation and hyperglycemia in mice. *J. Biol. Chem.* **284,** 8359–8368
10. Jenkins, R. W., Canals, D., and Hannun, Y. A. (2009) Roles and regulation of secretory and lysosomal acid sphingomyelinase. *Cell. Signal.* **21,** 836–846
11. Hannun, Y. A. (1996) Functions of ceramide in coordinating cellular responses to stress. *Science* **274,** 1855–1859
12. Summers, S. A., and Nelson, D. H. (2005) A role for sphingolipids in producing the common features of type 2 diabetes, metabolic syndrome X, and Cushing's syndrome. *Diabetes* **54,** 591–602
13. Holland, W. L., Brozinick, J. T., Wang, L. P., Hawkins, E. D., Sargent, K. M., Liu, Y., Narra, K., Hoehn, K. L., Knotts, T. A., Siesky, A., Nelson, D. H., Karathanasis, S. K., Fontenot, G. K., Birnbaum, M. J., and Summers, S. A. (2007) Inhibition of ceramide synthesis ameliorates glucocorticoid-, saturated-fat-, and obesity-induced insulin resistance. *Cell Metab.* **5,** 167–179
14. Holland, W. L., and Summers, S. A. (2008) Sphingolipids, insulin resistance, and metabolic disease: new insights from in vivo manipulation of sphingolipid metabolism. *Endocr. Rev.* **29,** 381–402
15. Wymann, M. P., and Schneiter, R. (2008) Lipid signalling in disease. *Nat. Rev. Mol. Cell Biol.* **9,** 162–176
16. Stratford, S., DeWald, D. B., and Summers, S. A. (2001) Ceramide dissociates 3′-phosphoinositide production from pleckstrin homology domain translocation. *Biochem. J.* **354,** 359–368
17. Liangpunsakul, S., Sozio, M. S., Shin, E., Zhao, Z., Xu, Y., Ross, R. A., Zeng, Y., and Crabb, D. W. Inhibitory effect of ethanol on AMPK phosphorylation is mediated in part through elevated ceramide levels. *Am. J. Physiol. Gastrointest. Liver Physiol.* **298,** G1004–G1012
18. Tani, M., Ito, M., and Igarashi, Y. (2007) Ceramide/sphingosine/sphingosine 1-phosphate metabolism on the cell surface and in the extracellular space. *Cell. Signal.* **19,** 229–237
19. Osawa, Y., Banno, Y., Nagaki, M., Brenner, D. A., Naiki, T., Nozawa, Y., Nakashima, S., and Moriwaki, H. (2001) TNF-α-induced sphingosine 1-phosphate inhibits apoptosis through a phosphatidylinositol 3-kinase/Akt pathway in human hepatocytes. *J. Immunol.* **167,** 173–180
20. Osawa, Y., Uchinami, H., Bielawski, J., Schwabe, R. F., Hannun, Y. A., and Brenner, D. A. (2005) Roles for C16-ceramide and sphingosine 1-phosphate in regulating hepatocyte apoptosis in response to tumor necrosis factor-α. *J. Biol. Chem.* **280,** 27879–27887
21. Rapizzi, E., Taddei, M. L., Fiaschi, T., Donati, C., Bruni, P., and Chiarugi, P. (2009) Sphingosine 1-phosphate increases glucose uptake through trans-activation of insulin receptor. *Cell. Mol. Life Sci.* **66,** 3207–3218
22. Osawa, Y., Hannun, Y. A., Proia, R. L., and Brenner, D. A. (2005) Roles of AKT and sphingosine kinase in the antiapoptotic effects of bile duct ligation in mouse liver. *Hepatology* **42,** 1320–1328
23. Allende, M. L., Sasaki, T., Kawai, H., Olivera, A., Mi, Y., van Echten-Deckert, G., Hajdu, R., Rosenbach, M., Keohane, C. A., Mandala, S., Spiegel, S., and Proia, R. L. (2004) Mice deficient in sphingosine kinase 1 are rendered lymphopenic by FTY720. *J. Biol. Chem.* **279,** 52487–52492
24. Adachi, M., and Brenner, D. A. (2008) High molecular weight adiponectin inhibits proliferation of hepatic stellate cells via activation of adenosine monophosphate-activated protein kinase. *Hepatology* **47,** 677–685

25. Bligh, E.G., and Dyer, W. J. (1959) A rapid method of total lipid extraction and purification. *Can. J. Biochem. Physiol.* **37,** 911–917
26. Pettus, B. J., Bielawski, J., Porcelli, A. M., Reames, D. L., Johnson, K. R., Morrow, J., Chalfant, C. E., Obeid, L. M., and Hannun, Y. A. (2003) The sphingosine kinase 1/sphingosine-1-phosphate pathway mediates COX-2 induction and PGE_2 production in response to TNF-α. *FASEB J.* **17,** 1411–1421
27. Gonzalez, A. A., Kumar, R., Mulligan, J. D., Davis, A. J., Weindruch, R., and Saupe, K. W. (2004) Metabolic adaptations to fasting and chronic caloric restriction in heart, muscle, and liver do not include changes in AMPK activity. *Am. J. Physiol. Endocrinol. Metab.* **287,** E1032–E1037
28. Wojtaszewski, J. F., Jorgensen, S. B., Hellsten, Y., Hardie, D. G., and Richter, E. A. (2002) Glycogen-dependent effects of 5-aminoimidazole-4-carboxamide (AICA)-riboside on AMP-activated protein kinase and glycogen synthase activities in rat skeletal muscle. *Diabetes* **51,** 284–292
29. Zang, M., Zuccollo, A., Hou, X., Nagata, D., Walsh, K., Herscovitz, H., Brecher, P., Ruderman, N. B., and Cohen, R. A. (2004) AMP-activated protein kinase is required for the lipid-lowering effect of metformin in insulin-resistant human HepG2 cells. *J. Biol. Chem.* **279,** 47898–47905
30. Grassme, H., Gulbins, E., Brenner, B., Ferlinz, K., Sandhoff, K., Harzer, K., Lang, F., and Meyer, T. F. (1997) Acidic sphingomyelinase mediates entry of *N. gonorrhoeae* into nonphagocytic cells. *Cell* **91,** 605–615
31. Pyne, S., and Pyne, N. J. (2002) Sphingosine 1-phosphate signalling and termination at lipid phosphate receptors. *Biochim. Biophys. Acta* **1582,** 121–131
32. Olivera, A., and Spiegel, S. (1993) Sphingosine-1-phosphate as second messenger in cell proliferation induced by PDGF and FCS mitogens. *Nature* **365,** 557–560
33. Siehler, S., and Manning, D. R. (2002) Pathways of transduction engaged by sphingosine 1-phosphate through G protein-coupled receptors. *Biochim. Biophys. Acta* **1582,** 94–99
34. Yang, A. H., Ishii, I., and Chun, J. (2002) In vivo roles of lysophospholipid receptors revealed by gene targeting studies in mice. *Biochim. Biophys. Acta* **1582,** 197–203
35. Hardie, D. G. (2007) AMP-activated/SNF1 protein kinases: conserved guardians of cellular energy. *Nat. Rev. Mol. Cell Biol.* **8,** 774–785
36. Leclerc, I., Lenzner, C., Gourdon, L., Vaulont, S., Kahn, A., and Viollet, B. (2001) Hepatocyte nuclear factor-4α involved in type 1 maturity-onset diabetes of the young is a novel target of AMP-activated protein kinase. *Diabetes* **50,** 1515–1521
37. Hou, X., Xu, S., Maitland-Toolan, K. A., Sato, K., Jiang, B., Ido, Y., Lan, F., Walsh, K., Wierzbicki, M., Verbeuren, T. J., Cohen, R. A., and Zang, M. (2008) SIRT1 regulates hepatocyte lipid metabolism through activating AMP-activated protein kinase. *J. Biol. Chem.* **283,** 20015–20026
38. Wu, Y., Song, P., Xu, J., Zhang, M., and Zou, M. H. (2007) Activation of protein phosphatase 2A by palmitate inhibits AMP-activated protein kinase. *J. Biol. Chem.* **282,** 9777–9788
39. Igarashi, J., Shoji, K., Hashimoto, T., Moriue, T., Yoneda, K., Takamura, T., Yamashita, T., Kubota, Y., and Kosaka, H. (2009) Transforming growth factor-β1 down-regulates caveolin-1 expression and enhances sphingosine 1-phosphate signaling in cultured vascular endothelial cells. *Am. J. Physiol. Cell Physiol* **297,** C1263–C1274
40. Adams, J. M., 2nd, Pratipanawatr, T., Berria, R., Wang, E., DeFronzo, R. A., Sullards, M. C., and Mandarino, L. J. (2004) Ceramide content is increased in skeletal muscle from obese insulin-resistant humans. *Diabetes* **53,** 25–31
41. Glimcher, L. H., and Lee, A. H. (2009) From sugar to fat: How the transcription factor XBP1 regulates hepatic lipogenesis. *Ann. N. Y. Acad. Sci.* **1173**(Suppl. 1), E2–E9
42. Stiles, B., Wang, Y., Stahl, A., Bassilian, S., Lee, W. P., Kim, Y.-J., Sherwin, R., Devaskar, S., Lesche, R., Magnuson, M. A., and Wu, H. (2004) Live-specific deletion of negative regulator Pten results in fatty liver and insulin hypersensitivity. *Proc. Natl. Acad. Sci. U. S. A.* **101,** 2082–2087
43. Watson, R. T., Shigematsu, S., Chiang, S. H., Mora, S., Kanzaki, M., Macara, I. G., Saltiel, A. R., and Pessin, J. E. (2001) Lipid raft microdomain compartmentalization of TC10 is required for insulin signaling and GLUT4 translocation. *J. Cell Biol.* **154,** 829–840
44. Sebastian, B. M., and Nagy, L. E. (2005) Decreased insulin-dependent glucose transport by chronic ethanol feeding is associated with dysregulation of the Cbl/TC10 pathway in rat adipocytes. *Am. J. Physiol. Endocrinol. Metab.* **289,** E1077–E1084
45. Zeidan, Y. H., and Hannun, Y. A. (2010) The acid sphingomyelinase/ceramide pathway: biomedical significance and mechanisms of regulation. *Curr. Mol. Med.* **10,** 454–466

Received for publication July 23, 2010.
Accepted for publication December 2, 2010.

J Gastroenterol (2011) 46:545–555
DOI 10.1007/s00535-010-0358-6

ORIGINAL ARTICLE—LIVER, PANCREAS, AND BILIARY TRACT

Factors predictive of sustained virological response following 72 weeks of combination therapy for genotype 1b hepatitis C

Kazuaki Chayama · C. Nelson Hayes · Kentaro Yoshioka · Hisataka Moriwaki · Takashi Okanoue · Shotaro Sakisaka · Tetsuo Takehara · Makoto Oketani · Joji Toyota · Namiki Izumi · Yoichi Hiasa · Akihiro Matsumoto · Hideyuki Nomura · Masataka Seike · Yoshiyuki Ueno · Hiroshi Yotsuyanagi · Hiromitsu Kumada

Received: 1 November 2010 / Accepted: 25 November 2010 / Published online: 19 January 2011

Abstract
Background Treatment of genotype 1b chronic hepatitis C virus (HCV) infection has been improved by extending peg-interferon plus ribavirin combination therapy to 72 weeks, but predictive factors are needed to identify those patients who are likely to respond to long-term therapy.
Methods We analyzed amino acid (aa) substitutions in the core protein and the interferon sensitivity determining region (ISDR) of nonstructural protein (NS) 5A in 840 genotype 1b chronic hepatitis C patients with high viral load. We used logistic regression and classification and regression tree (CART) analysis to identify predictive factors for sustained virological response (SVR) for patients undergoing 72 weeks of treatment.
Results When patients were separately analyzed by treatment duration using multivariate logistic regression, several factors, including sex, age, viral load, and core aa70 and ISDR substitutions ($P = 0.0003$, $P = 0.02$, $P = 0.01$, $P = 0.0001$, and $P = 0.0004$, respectively) were significant predictive factors for SVR with 48 weeks of treatment, whereas age, previous interferon treatment history, and ISDR substitutions ($P = 0.03$, $P = 0.01$, and $P = 0.02$,

Electronic supplementary material The online version of this article (doi:10.1007/s00535-010-0358-6) contains supplementary material, which is available to authorized users.

K. Chayama (✉) · C. N. Hayes
Department of Medical and Molecular Science,
Division of Frontier Medical Science,
Programs for Biomedical Research,
Graduate School of Biomedical Sciences,
Hiroshima University, 1-2-3 Kasumi, Minami-ku,
Hiroshima 734-8551, Japan
e-mail: chayama@hiroshima-u.ac.jp

K. Yoshioka
Division of Liver, Biliary Tract and Pancreas Diseases,
Department of Internal Medicine,
Fujita Health University, Nagoya, Japan

H. Moriwaki
Department of Gastroenterology,
Gifu University Graduate School of Medicine, Gifu, Japan

T. Okanoue
Department of Gastroenterology and Hepatology,
Saiseikai Suita Hospital, Suita, Japan

S. Sakisaka
Department of Gastroenterology and Medicine,
Fukuoka University School of Medicine, Fukuoka, Japan

T. Takehara
Department of Gastroenterology and Hepatology,
Osaka University Graduate School of Medicine, Osaka, Japan

M. Oketani
Department of Digestive and Life-Style Related Disease,
Health Research Course, Human and Environmental Sciences,
Kagoshima University Graduate School of Medical and Dental Sciences, Kagoshima, Japan

J. Toyota
Department of Gastroenterology,
Sapporo Kosei General Hospital, Sapporo, Japan

N. Izumi
Division of Gastroenterology and Hepatology,
Musashino Red Cross Hospital, Musashino, Japan

Y. Hiasa
Department of Gastroenterology and Metabology,
Ehime University Graduate School of Medicine,
Matsuyama, Japan

respectively) were the only significant predictive factors with 72 weeks of treatment. Using CART analysis, a decision tree was generated that identified age, cholesterol, sex, treatment length, and aa70 and ISDR substitutions as the most important predictive factors. The CART model had a sensitivity of 69.2% and specificity of 60%, with a positive predictive value of 68.4%.

Conclusions Complementary statistical and data mining approaches were used to identify a subgroup of patients likely to benefit from 72 weeks of therapy.

Keywords CART analysis · Core protein · Decision tree · ISDR · LDL cholesterol

Abbreviations

HCV	Hepatitis C virus
ISDR	Interferon sensitivity determining region
CART	Classification and regression tree analysis
SVR	Sustained virological response
NR	Non-viral response

Introduction

Chronic hepatitis C virus (HCV) infection is a major global cause of chronic hepatitis, liver cirrhosis, and hepatocellular carcinoma [1–3]. The treatment of chronic hepatitis C has improved with the advent of peg-interferon (IFN) plus ribavirin combination therapy [4–7], but fewer than half of the patients with high viral loads of genotype 1b show a sustained virological response (SVR), defined as testing negative for HCV RNA 24 weeks after cessation of the therapy. To overcome this limitation, recent therapeutic regimens have extended the treatment period to 72 weeks [8–11]. This extension is especially effective in patients whose HCV RNA declines relatively slowly [9–11]. Accordingly, recent treatment protocols have recommended extending the treatment period to 72 weeks in patients who become negative for HCV RNA after 12 weeks of treatment but before 24 weeks [10, 11]. This response-guided decision-making approach to therapy has resulted in improvements of the SVR rate [10, 11]. Following this approach, patients with a non-viral response (NR), i.e., patients who show very poor response to the therapy (defined as less than 2-log decline of HCV RNA during 12 weeks of treatment), should be advised to discontinue therapy because SVR is rare in such patients. While response-guided therapy is useful in determining the appropriate duration of treatment for patients who are likely to respond eventually, predictors that can be assessed before the start of therapy will aid in differentiating which difficult-to-treat patients are likely to achieve an SVR with extended therapy and which may be better served by considering alternative therapy options.

To predict NR, recent studies recommend analysis of amino acid (aa) substitutions in the HCV core protein at positions 70 and 91 [12, 13]. The substitution of arginine with glutamine or other amino acids at core protein aa 70 has been reported to be associated with NR, and this finding was confirmed by several other groups [14–16]. Analysis of core aa 70 has also been shown to be useful to predict the outcome of 72 weeks of combination therapy [17]. While many factors have been reported to be useful predictors of the effect of combination therapy [18–26], many of these factors are mutually interdependent. Furthermore, because almost all of these factors have been reported under conditions in which a majority of patients were receiving 48 weeks of treatment, it is necessary to consider the effect of the treatment period.

In this study, we compiled a database of clinical data from 840 patients from 16 national centers in Japan. We used logistic regression and classification and regression tree analysis (CART) to identify factors predictive of SVR for 48- and 72-week therapy and to assess which patients are most likely to benefit by long-term 72-week therapy.

Methods

Study subjects

In this retrospective study, data from 840 patients with chronic hepatitis C treated at 16 different hospitals in Japan were analyzed for predictive factors for SVR based on

A. Matsumoto
Department of Medicine, Shinshu University School of Medicine, Matsumoto, Japan

H. Nomura
The Center for Liver Diseases, Shin-Kokura Hospital, Kokura, Japan

M. Seike
Department of Internal Medicine 1, Faculty of Medicine, Oita University, Oita, Japan

Y. Ueno
Division of Gastroenterology, Tohoku University Graduate School of Medicine, Sendai, Japan

H. Yotsuyanagi
Department of Internal Medicine, Graduate School of Medicine, University of Tokyo, Tokyo, Japan

H. Kumada
Department of Hepatology, Toranomon Hospital, Tokyo, Japan

Table 1 Patient characteristics for 48- and 72-week treatments

	All patients ($n = 840$)	48-Week therapy ($n = 619$) 73.69%	72-Week therapy ($n = 221$) 25.12%
Age (years)	54.4 ± 10.73	53.8 ± 11.21	56.2 ± 9.03
Gender (male/female)	449/391	357/262	92/129
Body weight (kg)	60.9 ± 10.8	61.3 ± 10.6	59.8 ± 11.4
Height (cm)	162.2 ± 9.1	162.7 ± 9.1	160.7 ± 9.0
BMI	23.0 ± 3.05	23.0 ± 2.92	23.0 ± 3.4
HCV core protein aa 70 (wild/mutant)	539/301	396/223	143/78
HCV core protein aa 91 (wild/mutant)	504/336	369/250	135/86
ISDR (0–1/≥2)	714/126	513/106	201/20
Hypertension (present/absent/ND)	538/113/189	395/78/146	143/35/43
Diabetes (present/absent/ND)	634/47/159	457/38/124	177/9/35
Transfusion (present/absent/ND)	505/227/108	379/162/78	126/65/30
Fibrosis stage (0–2/3–4/ND)	604/128/108	448/90/81	156/38/27
Activity stage (0–1/2–3/ND)	382/343/115	287/245/87	95/98/28
Steatosis (present/absent/ND)	158/344/338	119/250/250	39/94/88
AST (IU/l)	65 ± 49	66 ± 47	63 ± 53
ALT (IU/l)	68 ± 56	68 ± 56	66 ± 55
White blood cell count (/mm^3)	4832 ± 1455	4882 ± 1488	4693 ± 1352
Hemoglobin (g/dl)	14.2 ± 1.36	14.3 ± 1.39	14.1 ± 1.29
Platelets ($\times 10^4$/mm^3)	16.9 ± 5.18	17.0 ± 5.11	16.8 ± 5.35
γGTP (IU/l)	56 ± 59	59 ± 64	49 ± 42
Albumin (g/dl)	4.02 ± 0.348	4.01 ± 0.350	4.03 ± 0.343
Uric acid (mg/dl)	5.41 ± 1.29	5.46 ± 1.27	5.25 ± 1.35
Iron (μg/dl)	147.0 ± 69.65	151.0 ± 75.71	136.1 ± 47.45
Ferritin (μg/l)	173.9 ± 167.9	181.7 ± 175.7	153.0 ± 143.7
Fasting blood sugar (mg/dl)	99.8 ± 19.8	99.3 ± 19.1	101.2 ± 21.5
Alpha-fetoprotein (μg/l)	16.3 ± 50.4	14.2 ± 44.8	22.0 ± 62.7
Total cholesterol (mg/dl)	175 ± 32.3	173 ± 31.8	179 ± 33.4
LDL cholesterol (mg/dl)	100.8 ± 29.8	100.2 ± 30.3	102.5 ± 28.4
HDL cholesterol (mg/dl)	52.1 ± 15.5	51.4 ± 15.0	53.9 ± 16.6
Triglycerides (mg/dl)	103.2 ± 48.8	103.8 ± 46.1	101.7 ± 55.1
HCV-RNA (KIU/ml)	3239 ± 4669	3170 ± 4828	3427 ± 4205
Response to treatment (SVR/TR/NR)	465/246/129	341/164/114	124/82/15

BMI body mass index, *HCV* hepatitis C virus, *aa* amino acid, *ISDR* interferon sensitivity determining region, *AST* aspartate aminotransferase, *ALT* alanine aminotransferase, *γGTP* γ-glutamyl transpeptidase, *LDL* low-density lipoprotein, *HDL* high-density lipoprotein, *SVR* sustained virological response, *TR* transient response/relapsers, *NR* non-viral response, *ND* not determined

treatment duration. Inclusion criteria included testing positive for HCV RNA for longer than 6 months and testing negative for both hepatitis B virus surface antigen and anti-HIV antibody. Patients with confounding conditions such as hemochromatosis, Wilson's disease, primary biliary cirrhosis, alcoholic liver disease, and autoimmune liver disease were excluded. We excluded patients who were lost for follow up and those who did not show a high level of viremia for genotype 1b, as well as patients for whom we failed to determine both core and IFN sensitivity determining region (ISDR) of nonstructural protein (NS) 5A sequences; 385 patients were treatment-naïve. All subjects gave their written informed consent to participate in the study according to the process approved by the ethics committee of each hospital and conforming to the ethical guidelines of the 1975 Declaration of Helsinki. Patient profiles are listed in Table 1.

All patients initially received weekly injections of peg-IFN-alpha-2b for 48 weeks (60 μg for body weight (BW) 35–45 kg, 80 μg for BW 46–60 kg, 100 μg for BW 61–75 kg, 120 μg for BW 76–90 kg, and 150 μg for BW 91–120 kg). Ribavirin was administered orally, and the dosage was determined based on the patient's BW (600 mg for <60 kg, 800 mg for 60–80 kg, and 1,000 mg

for >80 kg). Ribavirin dosage was reduced when hemoglobin levels were reduced to 10.0 g/dl and stopped if hemoglobin levels reached 8.5 g/dl. Successful treatment was ascertained based on SVR, defined as HCV RNA-negative 6 months after cessation of therapy. Using response-guided therapy, slow viral responders, i.e., patients for whom HCV RNA levels became negative after 12 weeks of therapy but before 24 weeks, and some non-responders were recommended for extension of therapy to 72 weeks.

Biochemical tests were performed at the individual hospitals, and pathological diagnosis was made by pathologists in each hospital according to the criteria of Desmet et al. [27]. Fibrosis and activity data were compared among hospitals to ensure that there were no systematic differences.

Analysis of viral titer and amino acid sequences in the core and ISDR region

The HCV RNA level was analyzed using reverse transcription polymerase chain reaction (RT-PCR)-based methods (Amplicor^{TM} high-range test; Roche Diagnostics, Basel, Switzerland, or TaqMan RT-PCR test; Applied Biosystems, CA). The measurement ranges of these assays were 5–5000 KIU/ml and 1.2–7.8 log IU/ml, respectively. For values exceeding the measurable range, the limit value was used as an approximation. The values obtained by the Amplicor test were converted to logarithmic values [28].

Nucleotide and amino acid sequences of the core and the ISDR region were determined by direct sequencing of cDNA fragments amplified by PCR. Arginine and leucine were considered wild-type for core protein aa 70 and aa 91, respectively [12, 13]. The number of aa substitutions in the ISDR was determined by comparison with the reference sequence reported by Kato et al. [29] using the method of Enomoto et al. [30, 31].

Statistical analysis

Statistical analysis was performed using the R software package (http://www.r-project.org). The χ^2 or Fisher's exact and Mann–Whitney U-tests were used to detect significant associations. All statistical analyses were two-sided, and $P < 0.05$ was considered significant. Simple and multiple logistic regression analyses were used to examine the association between viral substitutions and clinical factors, using $P < 0.05$ as the criterion for inclusion in the initial multivariate model. Multivariate logistic regression analysis was performed using forward/backward stepwise selection based on the akaike information criterion (AIC) score and validated by bootstrapping, using the rms package in R. Odds ratios (ORs) and 95% confidence intervals (CIs) were calculated for each factor.

CART analysis

CART analysis was used to generate a decision tree by classifying patients by SVR, based on a recursive partitioning algorithm with minimal cost-complexity pruning to identify optimal classification factors. The SimpleCart classifier in the WEKA data mining package [32] was used with a minimal terminal node size of 4 and trained with the variables listed in Table 1. Performance was assessed using tenfold cross-validation, and the sensitivity, specificity, and precision of the model were calculated. Receiver operating characteristic (ROC) curves were generated and results were compared with the logistic regression model.

Results

Patient characteristics

Patients were partitioned into two groups based on whether they received 48 or 72 weeks of therapy (Table 1). In this study 465 patients achieved an SVR, whereas 375 patients were either non-responders or relapsers, yielding an overall SVR rate of 55.4%. The rate of SVR did not differ significantly between the 48- and 72-week treatment groups (55.3 vs. 56.4%, respectively; $P = 0.81$), but the NR rate was significantly lower in patients who were treated for 72 weeks (18.3 vs. 6.4%; $P = 9.3 \times 10^{-6}$).

Predictive factors for SVR

The association between SVR and individual clinical factors was assessed using logistic regression. A number of factors were significant at the $P < 0.05$ level, including age, sex, viral load, aa70/ISDR substitutions, hypertension, fibrosis, steatosis, prior IFN treatment, low-density lipoprotein (LDL) cholesterol, total cholesterol, white blood cell count, platelet count, hemoglobin, γ-glutamyl transpeptidase (γGTP), and albumin (Table 2). On multivariate logistic regression, only age, sex, core aa70, ISDR, LDL, and γGTP were identified as significant independent predictors of SVR. Although length of treatment was not identified as a significant predictor in this analysis, exploratory analysis suggests the presence of potential interactions between treatment length and age and/or sex that are not captured by the first-order terms in the model. When second-order terms were selected a posteriori, however, a significant interaction was found between sex and treatment length ($P = 0.0034$). When analyzed separately, independent predictive factors for SVR for 48 weeks

Table 2 Factors associated with sustained virological response to combination therapy

Variable	Simple			Multiple			
	n	OR	*P*	*n*	OR	(95% CI)	*P*
Age	840	0.393	3.16×10^{-11}***	517	0.386	(0.27–0.56)	5.08×10^{-7}***
Sex (male vs. female)	840	0.521	3.61×10^{-6}***	517	0.52	(0.35–0.78)	0.001459**
BMI (kg/m^2)	834	0.8	0.1094				
Viral load (Log IU/ml)	840	0.761	0.001828**				
Core aa70 substitution	840	0.537	1.98×10^{-5}***	517	0.507	(0.35–0.74)	0.000521***
Core aa91 substitution	840	0.818	0.1568				
ISDR (0–1 vs. ≥2)	840	2.36	5.19×10^{-5}***	517	2.12	(1.19–3.77)	0.01037*
Hypertension	651	0.625	0.02389*				
Diabetes	681	0.794	0.4464				
Blood transfusion	732	1	0.9788				
Fibrosis (F0–1 vs. F2–4)	732	0.674	0.008287**				
Activity (A0–1 vs. A2–4)	725	0.779	0.09567				
Steatosis	502	0.645	0.03413*				
Prior IFN treatment	830	1.37	0.02648*				
HDL cholesterol (mg/dl)	493	0.761	0.1333				
LDL cholesterol (mg/dl)	529	1.46	0.03223*	517	1.61	(1.10–2.38)	0.01521*
Triglyceride (mg/dl)	726	0.913	0.5412				
Total cholesterol (mg/dl)	814	1.25	0.11				
AST (IU/l)	783	0.933	0.6316				
ALT (IU/l)	840	0.972	0.837				
WBC (/mm^3)	836	1.55	0.001831**				
Hemoglobin (g/dl)	838	1.34	0.00276**				
Platelets ($\times 10^4$/mm^3)	838	1.74	7.92×10^{-5}***				
Gamma-GTP (IU/l)	823	0.735	0.0288*	517	0.656	(0.43–0.99)	0.04588*
Albumin (g/dl)	809	1.41	0.01699*				
Ferritin (μg/l)	532	0.898	0.5404				
Treatment period (weeks)	840	1.02	0.6095				

Simple and multiple logistic regression was used to examine the association between SVR and patient and viral factors. Factors with $P < 0.05$ were considered for inclusion in the multiple regression model and the best model selected by backwards stepwise selection using AIC

*** $P < 0.001$, ** $P < 0.01$, * $P < 0.05$

IFN interferon, *OR* odds ratio, *CI* confidence interval, *AIC* akaike information criterion

of treatment included age, sex, viral load, core aa70, LDL, platelets, and white blood cell counts, whereas for 72 weeks of treatment only age, ISDR, and prior IFN treatment were significant, although LDL cholesterol was marginally significant (Table 3).

Among patients who underwent 48 weeks of therapy, 61% of patients with core aa 70 wild-type achieved an SVR compared to only 44% of patients with mutant core aa 70 ($P = 1.8 \times 10^{-5}$, Fig. 1a), whereas for 72-week patients, the ratio was 1:1 (Fig. 3a). Conversely, in the 48-week group, 71% of patients with two or more mutations in the ISDR were able to achieve an SVR compared to 52% with the wild-type ISDR, and in the 72-week group (Fig. 1b), 80% of patients with two or more ISDR mutations achieved an SVR compared to 54% with zero or one ISDR mutations (Fig. 3b). Median baseline viral load was significantly lower in 48-week SVR patients compared to that in non-SVR patients ($P = 0.001$, Fig. 1c), whereas there was no significant difference between viral load and SVR in 72-week therapy patients ($P = 0.625$, Fig. 4c). There was a significant effect of age and treatment outcome among 48-week patients ($P = 9.3 \times 10^{-6}$, Fig. 2), but the difference was not significant among 72-week therapy patients. However, the proportion of patients achieving an SVR tended to decrease with age in both groups, particularly in females over age 70 years in the 72-week group (Figs. 2, 4).

Table 3 Independent factors associated with sustained virological response to 48- and 72-week peg-interferon plus ribavirin combination therapy

Variable	48 Weeks			72 Weeks			
	n	OR	*P*	*n*	OR	(95% CI)	*P*
Age	535	0.642	0.0165*	133	0.4	(0.176–0.91)	0.02877*
Sex (male vs. female)	535	0.481	0.000284**				
Viral load (Log IU/ml)	535	0.738	0.01033*				
Core aa70 substitution	535	0.454	9.95×10^{-5}**				
ISDR (0–1 vs. ≥2)	535	2.75	0.000358**	133	7	(1.35–36.2)	0.02047*
Fibrosis (F0–1 vs. F2–4)	535	0.66	0.03954*				
Prior IFN treatment				133	2.67	(1.22–5.85)	0.01431*
LDL cholesterol (mg/dl)				133	2.04	(0.952–4.35)	0.06673
WBC ($/mm^3$)	535	1.53	0.03342*				
Platelets ($\times 10^4/mm^3$)	535	1.54	0.03707*				

Simple and multiple logistic regression analysis was used to examine the association between SVR and patient/viral factors separately for patients receiving 48 and 72 weeks of treatment

** $P < 0.001$, * $P < 0.05$

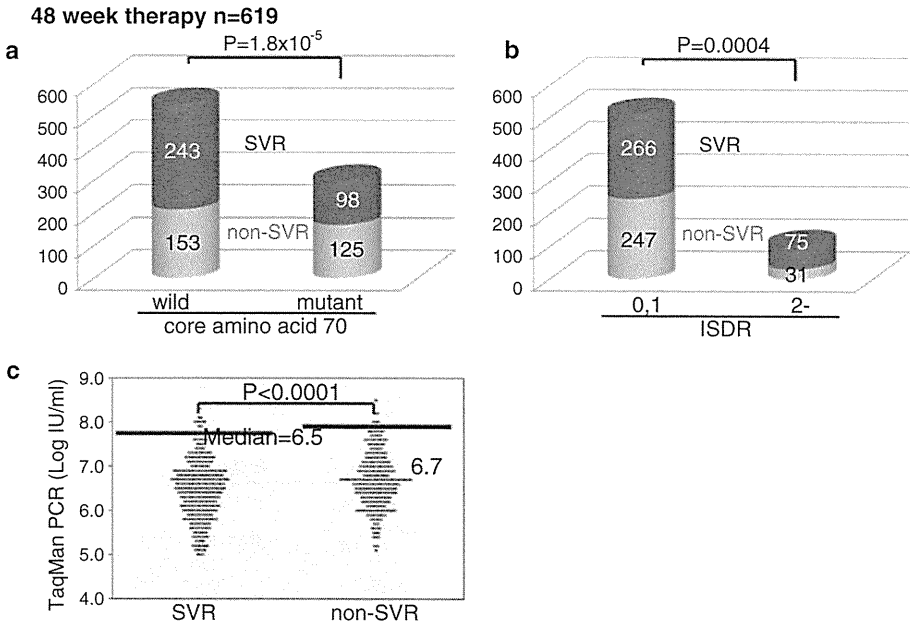

Fig. 1 Viral factors for 48-week treatment. Relationships between sustained virological response (*SVR*) and **a** core amino acid 70 substitutions, **b** amino acid substitutions in the interferon sensitivity determining region, and **c** baseline viral titers grouped by SVR and non-SVR for patients treated for 48 weeks. *PCR* Polymerase chain reaction

CART analysis

Figure 5 shows the decision tree generated by CART analysis. All variables were included during model construction, and the SimpleCart algorithm generated a tree based on the following fields: age, cholesterol, sex, γGTP, 48 versus 72 weeks of treatment, and aa substitutions in the ISDR and at core aa70. Age was used as the first cutoff, and patients younger than 46.5 years were classified as having a high probability for SVR (78%). Total cholesterol was identified as the next decision point, and patients with cholesterol higher than 211.5 mg/dl were classified as SVR if they were younger than 62.5 years (84%) and NR (65%) otherwise. Patients with cholesterol lower than 211.5 mg/dl were subdivided next by sex. Females who received 48 weeks of treatment were classified as NR (71%), whereas females receiving 72 weeks of treatment were classified as SVR if they were younger than 58.5 years (71%) or NR otherwise (64%). Males who were infected with aa70 wild-type were classified as SVR (62%), whereas males with aa70 substitutions were classified as NR if total cholesterol was less than 130 mg/dl (97%). Males with ISDR substitutions were classified as SVR (75%), and those with wild-type ISDR were classified

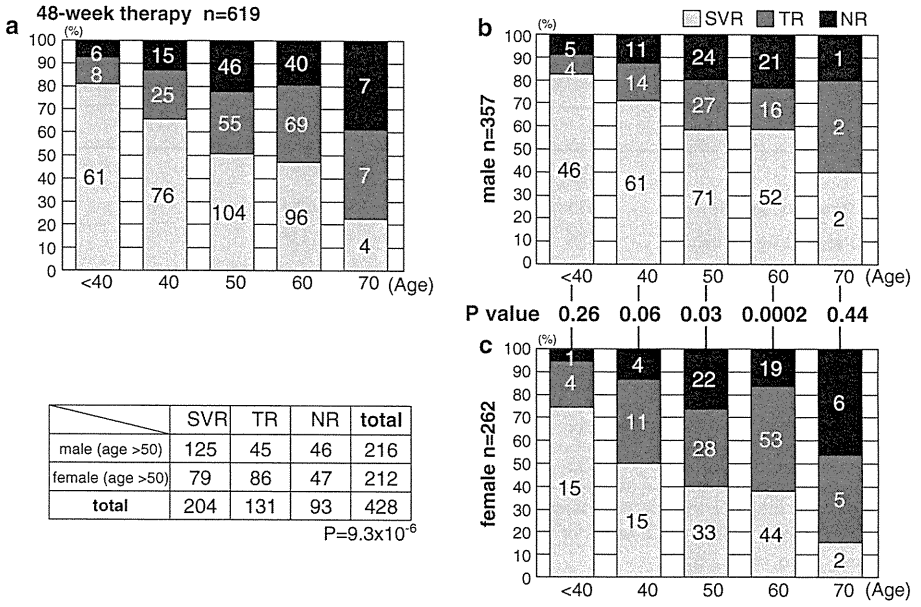

	SVR	TR	NR	total
male (age >50)	125	45	46	216
female (age >50)	79	86	47	212
total	204	131	93	428

$P=9.3\times10^{-6}$

Fig. 2 Relationship between age and response to treatment for 48-week therapy. Treatment outcomes by age in 10-year intervals are shown for **a** all patients, **b** males only, and **c** females only. *NR* non-viral response

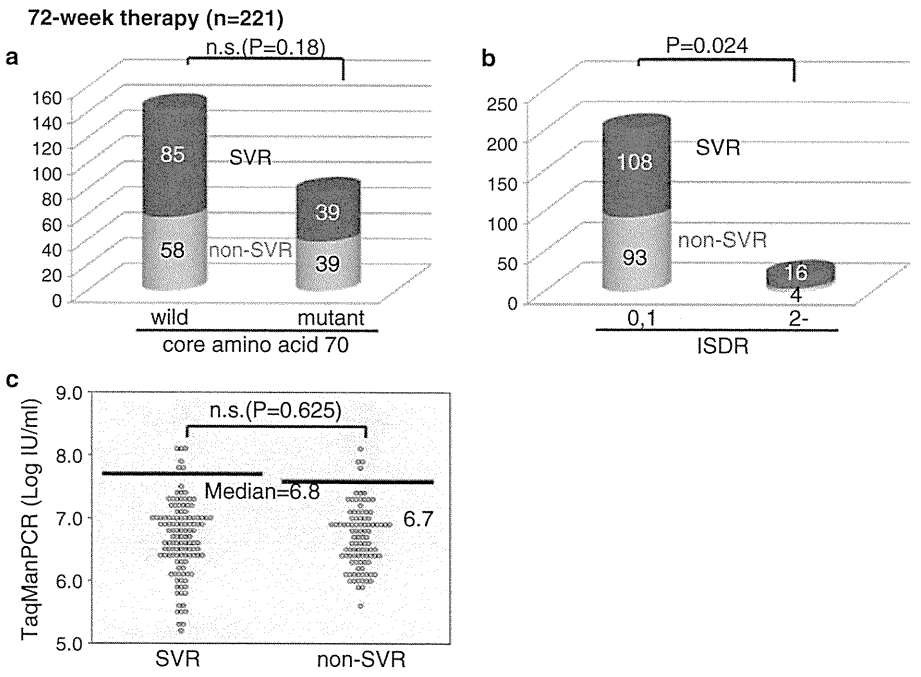

Fig. 3 Viral factors for 72-week treatment. Relationships between sustained virological response and **a** core amino acid 70 substitutions, **b** amino acid substitutions in the interferon sensitivity determining region, and **c** baseline viral titers grouped by SVR and non-SVR for patients treated for 72 weeks. *n.s.*, Not significant

as SVR if γGTP was less than 48.5 IU/l (57%) and NR otherwise (77%).

All factors selected during tree construction were found to be significant in univariate analysis, except for treatment length and cholesterol, and each remained significant in multivariate logistic regression. Although LDL was included in the multivariate logistic model, it was not selected during tree construction. Tenfold cross-validation resulted in 65.2% correctly classified instances with a kappa statistic of 0.29. The true positive rate was 69.2%, the false positive rate was 39.7%, and precision was 68.4%.

To compare the performance of SVR prediction between the logistic and CART models, the WEKA Logistic classifier was used to perform tenfold validation based on the

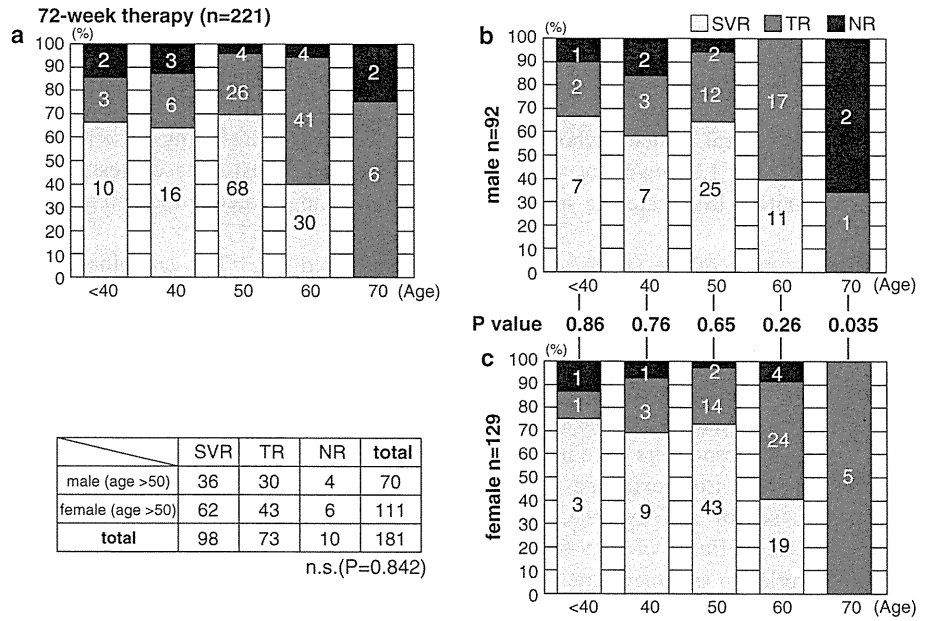

	SVR	TR	NR	total
male (age >50)	36	30	4	70
female (age >50)	62	43	6	111
total	98	73	10	181

n.s.(P=0.842)

Fig. 4 Relationship between age and response to treatment for 72-week therapy. Treatment outcomes by age in 10-year intervals are shown for **a** all patients, **b** males only, and **c** females only

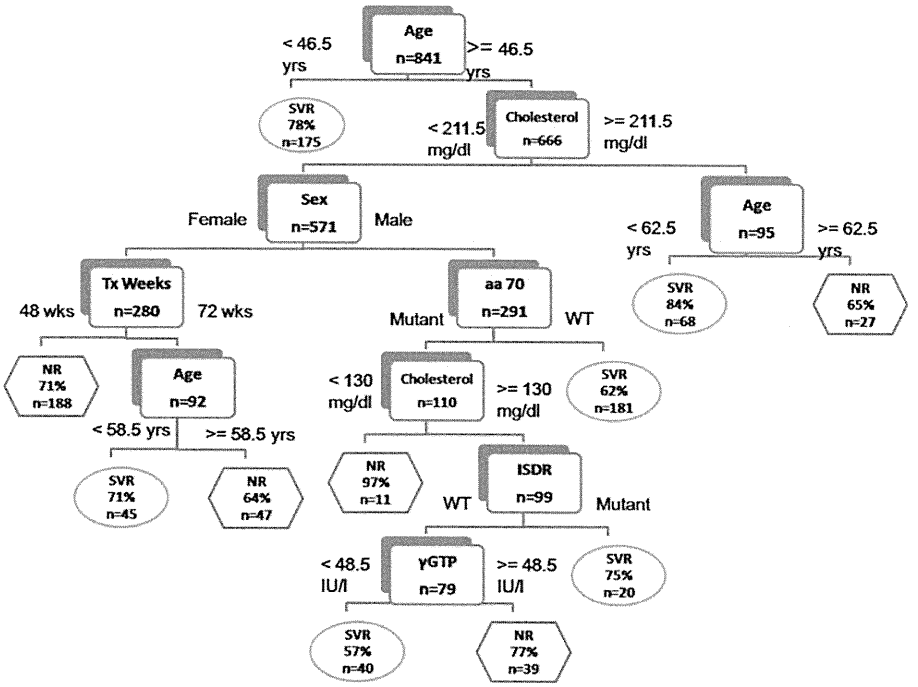

Fig. 5 Decision tree for SVR prediction. *Boxes* represent branch points based on cutoff values for factors determined by the tree generation algorithm. Each branch contains two choices, and each path ends in a prediction for either SVR or NR with an associated probability. *yrs* Years, *Tx* treatment, *ISDR* interferon sensitivity determining region, *aa* amino acid, *WT* wild-type, *γGTP* γ-glutamyl transpeptidase

multivariate logistic regression model above. The true positive rate for the logistic classifier was somewhat higher, at 73.1%, but with a slightly worse false-positive rate of 48%, and 63.7% correctly classified instances with a kappa statistic of 0.25 and precision 0.65. Receiver operating characteristic (ROC) curves were very similar, and the area under the curve was 0.677 for the CART model and 0.696 for the logistic model.

Discussion

Using two complementary approaches we identified several pretreatment factors predictive for SVR in patients treated for 48 and 72 weeks. Logistic regression and CART analysis both suggest that sex, age, cholesterol, and substitutions at core aa70 and ISDR are associated with SVR in patients with a high viral load of genotype 1b. Based on

the decision tree topology and a significant interaction between sex and treatment duration, it appears that 72 weeks of treatment may be most beneficial in women between the ages of 46 and 58 years who have low cholesterol. In general, patients who are younger, male, have cholesterol over 130 mg/dl, or who have wild-type core aa70 or mutant ISDR are the most likely to achieve an SVR.

Because each of the above values can be determined prior to treatment and are interpretable by clinicians, they may be useful as a guide when establishing a treatment regimen in the case of potentially difficult-to-treat patients. Once IFN treatment has been started, early and/or rapid viral response is likely to be the strongest predictor of SVR [33], and slow responders have been shown to be the most likely to benefit from extended treatment [34, 35]. However, because of the expense, low success rate, and potential side effects of IFN-based therapy, predictors available prior to treatment are also needed. Factors predictive of NR may help guide the decision to avoid or discontinue IFN therapy in patients with a low probability of SVR, and factors predictive of SVR may help identify subsets of patients who are likely to achieve an SVR if treated longer than the standard 48-week regimen.

Several other recent studies have examined predictors for SVR for 72 weeks of treatment, although nearly all focus on on-treatment predictors and conclude that 72-week therapy significantly improves SVR rates in slow responders [9, 10, 35]. Ferenci et al. [11] also showed that extension to 72 weeks decreased the relapse rate among early viral responders. In a large retrospective cohort study, Watanabe et al. [36] dissected a complex relationship between SVR and age, sex, and viral load similar to that reported here, although results are difficult to compare because they did not measure cholesterol or viral substitutions. While they recommend 72-week therapy for all slow-responding patients regardless of sex or age, they note that the SVR rate was surprisingly high among elderly female patients following 72-week treatment, noting that the SVR for 48-week treatment was typically low among older female patients in Japan, which they suggest could be related to the development of insulin resistance associated with menopause [36]. Other studies discourage the use of 72-week therapy for all patients except in the specific case of slow responders [8]. Moreover, in a large prospective study, Buti et al. [34] conclude that 48-week combination therapy should remain the standard of care even for slow responders, due to the increased cost and incidence of adverse events relative to a modest increase in the SVR rate. They clarify, however, that patients with a less than 2 log decline at week 8 and undetectable HCV RNA at week 24 are the most likely to benefit from 72-week treatment. Unfortunately they did not examine other predictors in a multivariate analysis. Because each of these studies hinges on rapid versus slow viral response and an on-treatment predictor requiring up to 24 weeks of treatment to establish, pretreatment predictors of early viral kinetics, including those presented here (e.g., viral substitutions and baseline cholesterol levels [12]), may be useful for predicting the outcome of extended therapy prior to treatment [17].

The combination of multiple approaches to identify predictive factors should help improve confidence in the results and partially protect against the bias inherent in any single approach. Comparing the results of a standard analysis with an alternative technique may reveal which variables are robust and which are sensitive to methodological differences. There are many different classification tools, including neural networks, Bayesian networks, and support vector machines, but models based on these may be more difficult to interpret or apply in clinical practice. On the other hand, decision tree approaches such as C4.5 and CART are widely used in biomedical studies [37–39] and provide a simple and intuitive hierarchical format that in many cases can be used without a computer.

The lack of randomized assignment of patients to duration of treatment limits the conclusions that can be drawn from the present study, and additional predictive factors, particularly interleukin (IL) 28B single-nucleotide polymorphism (SNP) genotype and viral kinetics, should be included in future prospective studies. Comparison of ROC curves suggests that the performance of the two models in the present study is similar, although neither is sufficiently sensitive or specific for accurate clinical prediction based on the number of patients analyzed. Nonetheless the strong overlap between the variables selected by each method suggests that several patient factors, including age, sex, and cholesterol level, as well as several viral factors, including core aa70 and ISDR substitutions, are robust predictors for SVR. Differences in the variables selected between the two approaches suggest that several models with similar predictive ability are also possible. In the regression model, LDL cholesterol but not total cholesterol was an independent factor associated with SVR, whereas in the CART analysis total cholesterol was selected instead. This may be due to the hierarchical nature of decision tree models, which may yield better results in the face of missing data, higher-order interactions, or nonlinear relationships. Comparison of separate models for 48 and 72 weeks also suggests that age and ISDR substitutions are important predictors of SVR for patients undergoing 72 weeks of treatment, whereas the decision tree suggests that the 72-week treatment length is important mainly for a subgroup of female patients. Without greater understanding of the role of HCV core and ISDR substitutions, it is difficult to interpret the role of these predictors, as well as

potential interactions with cholesterol level and other clinical factors. Further studies should be performed to investigate these interactions and to better characterize the subgroup of patients who are most likely to respond to long-term IFN therapy.

Acknowledgments This work was supported in part by Grants-in-Aid for scientific research and development from the Ministry of Health, Labor and Welfare and Ministry of Education, Culture, Sports, Science and Technology, Government of Japan. We thank Sakura Akamatsu and Mika Tsuzuno for their assistance.

Conflict of interest None of the authors have conflicts of interest to declare.

References

1. Hoofnagle JH. Hepatitis C: the clinical spectrum of disease. Hepatology. 1997;26:15S–20S.
2. Di Bisceglie AM. Hepatitis C. Lancet. 1998;351:351–5.
3. Marcellin P. Hepatitis C: the clinical spectrum of the disease. J Hepatol. 1999;31(Suppl 1):9–16.
4. Manns MP, McHutchison JG, Gordon SC, Rustgi VK, Shiffman M, Reindollar R, et al. Peginterferon alfa-2b plus ribavirin compared with interferon alfa-2b plus ribavirin for initial treatment of chronic hepatitis C: a randomised trial. Lancet. 2001;358:958–65.
5. Fried MW, Shiffman ML, Reddy KR, Smith C, Marinos G, Goncales FL Jr, et al. Peginterferon alfa-2a plus ribavirin for chronic hepatitis C virus infection. N Engl J Med. 2002;347:975–82.
6. Hadziyannis SJ, Sette H Jr, Morgan TR, Balan V, Diago M, Marcellin P, et al. Peginterferon-alpha2a and ribavirin combination therapy in chronic hepatitis C: a randomized study of treatment duration and ribavirin dose. Ann Intern Med. 2004;140:346–55.
7. Jensen DM, Marcellin P, Freilich B, Andreone P, Di Bisceglie A, Brandao-Mello CE, et al. Re-treatment of patients with chronic hepatitis C who do not respond to peginterferon-alpha2b: a randomized trial. Ann Intern Med. 2009;150:528–40.
8. Berg T, von Wagner M, Nasser S, Sarrazin C, Heintges T, Gerlach T, et al. Extended treatment duration for hepatitis C virus type 1: comparing 48 versus 72 weeks of peginterferon-alfa-2a plus ribavirin. Gastroenterology. 2006;130:1086–97.
9. Sanchez-Tapias JM, Diago M, Escartin P, Enriquez J, Romero-Gomez M, Barcena R, et al. Peginterferon-alfa2a plus ribavirin for 48 versus 72 weeks in patients with detectable hepatitis C virus RNA at week 4 of treatment. Gastroenterology. 2006;131:451–60.
10. Pearlman BL, Ehleben C, Saifee S. Treatment extension to 72 weeks of peginterferon and ribavirin in hepatitis C genotype 1-infected slow responders. Hepatology. 2007;46:1688–94.
11. Ferenci P, Laferl H, Scherzer TM, Maieron A, Hofer H, Stauber R, et al. Peginterferon alfa-2a/ribavirin for 48 or 72 weeks in hepatitis C genotypes 1 and 4 patients with slow virologic response. Gastroenterology. 2010;138:503–12. 12 e1.
12. Akuta N, Suzuki F, Kawamura Y, Yatsuji H, Sezaki H, Suzuki Y, et al. Predictive factors of early and sustained responses to peginterferon plus ribavirin combination therapy in Japanese patients infected with hepatitis C virus genotype 1b: amino acid substitutions in the core region and low-density lipoprotein cholesterol levels. J Hepatol. 2007;46:403–10.
13. Akuta N, Suzuki F, Sezaki H, Suzuki Y, Hosaka T, Someya T, et al. Predictive factors of virological non-response to interferon-ribavirin combination therapy for patients infected with hepatitis C virus of genotype 1b and high viral load. J Med Virol. 2006;78:83–90.
14. Okanoue T, Itoh Y, Hashimoto H, Yasui K, Minami M, Takehara T, et al. Predictive values of amino acid sequences of the core and NS5A regions in antiviral therapy for hepatitis C: a Japanese multi-center study. J Gastroenterol. 2009;44:952–63.
15. Mori N, Imamura M, Kawakami Y, Saneto H, Kawaoka T, Takaki S, et al. Randomized trial of high-dose interferon-alpha-2b combined with ribavirin in patients with chronic hepatitis C: correlation between amino acid substitutions in the core/NS5A region and virological response to interferon therapy. J Med Virol. 2009;81:640–9.
16. Ishii K, Shinohara M, Sawa M, Kogame M, Higami K, Sano M, et al. Interferon alpha receptor 2 expression by peripheral blood monocytes in patients with a high viral load of hepatitis C virus genotype 1 showing substitution of amino acid 70 in the core region. Intervirology. 2010;53:105–10.
17. Akuta N, Suzuki F, Hirakawa M, Kawamura Y, Yatsuji H, Sezaki H, et al. A matched case-controlled study of 48 and 72 weeks of peginterferon plus ribavirin combination therapy in patients infected with HCV genotype 1b in Japan: amino acid substitutions in HCV core region as predictor of sustained virological response. J Med Virol. 2009;81:452–8.
18. Sarrazin C, Herrmann E, Bruch K, Zeuzem S. Hepatitis C virus nonstructural 5A protein and interferon resistance: a new model for testing the reliability of mutational analyses. J Virol. 2002;76:11079–90.
19. Jenke AC, Moser S, Orth V, Zilbauer M, Gerner P, Wirth S. Mutation frequency of NS5A in patients vertically infected with HCV genotype 1 predicts sustained virological response to peginterferon alfa-2b and ribavirin combination therapy. J Viral Hepat. 2009;16:853–9.
20. Layden-Almer JE, Kuiken C, Ribeiro RM, Kunstman KJ, Perelson AS, Layden TJ, et al. Hepatitis C virus genotype 1a NS5A pretreatment sequence variation and viral kinetics in African American and white patients. J Infect Dis. 2005;192:1078–87.
21. Vuillermoz I, Khattab E, Sablon E, Ottevaere I, Durantel D, Vieux C, et al. Genetic variability of hepatitis C virus in chronically infected patients with viral breakthrough during interferon-ribavirin therapy. J Med Virol. 2004;74:41–53.
22. Puig-Basagoiti F, Forns X, Furcic I, Ampurdanes S, Gimenez-Barcons M, Franco S, et al. Dynamics of hepatitis C virus NS5A quasispecies during interferon and ribavirin therapy in responder and non-responder patients with genotype 1b chronic hepatitis C. J Gen Virol. 2005;86:1067–75.
23. Wohnsland A, Hofmann WP, Sarrazin C. Viral determinants of resistance to treatment in patients with hepatitis C. Clin Microbiol Rev. 2007;20:23–38.
24. El-Shamy A, Nagano-Fujii M, Sasase N, Imoto S, Kim SR, Hotta H. Sequence variation in hepatitis C virus nonstructural protein 5A predicts clinical outcome of pegylated interferon/ribavirin combination therapy. Hepatology. 2008;48:38–47.
25. El-Shamy A, Sasayama M, Nagano-Fujii M, Sasase N, Imoto S, Kim SR, et al. Prediction of efficient virological response to pegylated interferon/ribavirin combination therapy by NS5A sequences of hepatitis C virus and anti-NS5A antibodies in pretreatment sera. Microbiol Immunol. 2007;51:471–82.
26. Yang SS, Lai MY, Chen DS, Chen GH, Kao JH. Mutations in the NS5A and E2-PePHD regions of hepatitis C virus genotype 1b and response to combination therapy of interferon plus ribavirin. Liver Int. 2003;23:426–33.

27. Desmet VJ, Gerber M, Hoofnagle JH, Manns M, Scheuer PJ. Classification of chronic hepatitis—diagnosis, grading and staging. Hepatology. 1994;19:1513–20.
28. Chayama K, Suzuki F, Tsubota A, Akuta N, Someya T, Kobayashi M, et al. Evaluation of quantitative measurements of hepatitis C virus RNA to predict sustained response to interferon by genotype. J Virol Methods. 2001;95:33–45.
29. Kato N, Hijikata M, Ootsuyama Y, Nakagawa M, Ohkoshi S, Sugimura T, et al. Molecular cloning of the human hepatitis C virus genome from Japanese patients with non-A, non-B hepatitis. Proc Natl Acad Sci U S A. 1990;87:9524–8.
30. Enomoto N, Sakuma I, Asahina Y, Kurosaki M, Murakami T, Yamamoto C, et al. Comparison of full-length sequences of interferon-sensitive and resistant hepatitis-C virus 1b – sensitivity to interferon is conferred by amino-acid substitutions in the NS5A region. J Clin Invest. 1995;96:224–30.
31. Enomoto N, Sakuma I, Asahina Y, Kurosaki M, Murakami T, Yamamoto C, et al. Mutations in the nonstructural protein 5A gene and response to interferon in patients with chronic hepatitis C virus 1b infection. N Engl J Med. 1996;334:77–81.
32. Hall M, Frank E, Holmes G, Pfahringer B, Reutemann P, Witten IH. The WEKA data mining software: an update. SIGKDD Explor. 2009;11:10–8.
33. Zeuzem S, Berg T, Moeller B, Hinrichsen H, Mauss S, Wedemeyer H, et al. Expert opinion on the treatment of patients with chronic hepatitis C. J Viral Hepat. 2009;16:75–90.
34. Buti M, Lurie Y, Zakharova NG, Blokhina NP, Horban A, Teuber G, et al. Randomized trial of peginterferon alfa-2b and ribavirin for 48 or 72 weeks in patients with hepatitis C virus genotype 1 and slow virologic response. Hepatology. 2010;52:1201–7.
35. Farnik H, Lange CM, Sarrazin C, Kronenberger B, Zeuzem S, Herrmann E. Meta-analysis shows extended therapy improves response of patients with chronic hepatitis C virus genotype 1 infection. Clin Gastroenterol Hepatol. 2010;8:884–90.
36. Watanabe S, Enomoto N, Koike K, Izumi N, Takikawa H, Hashimoto E, et al. Prolonged treatment with pegylated interferon alpha 2b plus ribavirin improves sustained virological response in chronic hepatitis C genotype 1 patients with late response in a clinical real-life setting in Japan. Hepatol Res. 2010;40:135–44.
37. Kurosaki M, Matsunaga K, Hirayama I, Tanaka T, Sato M, Yasui Y, et al. A predictive model of response to peginterferon ribavirin in chronic hepatitis C using classification and regression tree analysis. Hepatol Res. 2010;40:251–60.
38. El Malki HO, El Mejdoubi Y, Souadka A, Mohsine R, Ifrine L, Abouqal R, et al. Predictive model of biliocystic communication in liver hydatid cysts using classification and regression tree analysis. BMC Surg. 2010;10:16.
39. Augustin S, Muntaner L, Altamirano JT, Gonzalez A, Saperas E, Dot J, et al. Predicting early mortality after acute variceal hemorrhage based on classification and regression tree analysis. Clin Gastroenterol Hepatol. 2009;7:1347–54.

MOLECULAR CANCER

RESEARCH Open Access

Dual induction of caspase 3- and transglutaminase-dependent apoptosis by acyclic retinoid in hepatocellular carcinoma cells

Hideki Tatsukawa[1], Tetsuro Sano[2], Yayoi Fukaya[1], Naoto Ishibashi[3], Makiko Watanabe[3], Masataka Okuno[4], Hisataka Moriwaki[4], Soichi Kojima[1*]

Abstract

Background: Hepatocellular carcinoma has a high mortality rate due to its rate of recurrence. Acyclic retinoid prevents recurrence of hepatocellular carcinoma in patients after surgical removal of their primary tumors by inducing apoptosis in hepatocellular carcinoma cells, although the molecular mechanisms of action are not understood.

Methods: Human hepatocellular carcinoma cells in culture, as well as nude mice transplanted with hepatocellular carcinoma cells and rats given with *N*-diethylnitrosamine were treated with acyclic retinoid. Changes in activated caspase 3 and transglutaminase 2 (TG2) levels, Sp1 cross-linking and its activities, expression of epidermal growth factor receptor, and apoptotic levels were measured.

Results: Acyclic retinoid simultaneously stimulated the activation of caspase 3, and the expression, nuclear localization and crosslinking activity of TG2, resulting in crosslinking and inactivation of the transcription factor, Sp1, thereby reducing expression of epidermal growth factor receptor and cell death in three hepatocellular carcinoma cell lines. These effects were partially restored by a caspase inhibitor, transfection of antisense TG2, restoration of functional Sp1, or an excess of epidermal growth factor. Nuclear expression of TG2 and crosslinked Sp1, as also activated caspase 3 were found in both hepatocellular carcinoma cells transplanted into nude mice and cancerous regions within the liver in *N*-diethylnitrosamine-induced hepatocarcinogenesis model in rats, following treatment of animals with acyclic retinoid.

Conclusions: Treatment with acyclic retinoid produces a dual activation of caspase 3 and TG2 induced apoptosis of hepatocellular carcinoma cells via modification and inactivation of Sp1, resulting in reduced expression of epidermal growth factor receptor.

Background

Hepatocellular carcinoma (HCC) has high mortality rate because of it frequent rate of recurrence [1]. Acyclic retinoid (ACR), a synthetic retinoid, prevents the recurrence and development of HCC in patients after surgical removal of the primary tumors by inducing apoptosis in HCC cells [2,3]. Retinoid X receptor (RXR) α is highly phosphorylated and loses its activity as a transcriptional factor during carcinogenesis in HCC [4]. ACR prevents this aberrant hyper-phosphorylation of RXRα by suppressing the Ras-extracellular signal regulated kinase (Erk) pathway, thereby restoring RXRα's activity in response to physiological concentrations of 9-*cis* retinoic acid (9-*cis* RA) [5]. We therefore proposed that this restoration of RXRα transcriptional activity is a basis for ACR's activity to control aberrant cell growth and induce apoptosis. However, the possibility that genes under the control of RARα/RXRv are upregulated by

* Correspondence: skojima@riken.jp
[1]Molecular Ligand Biology Research Team, Chemical Genomics Research Group, Chemical Biology Department, RIKEN Advanced Science Institute, Wako, Saitama 351-0198, Japan
Full list of author information is available at the end of the article

ACR, thereby mediating ACR's effect in suppressing aberrant growth and/or inducing apoptosis, has not been fully elucidated. ACR downregulates epidermal growth factor receptor (EGFR) signals due to suppression of transforming growth factor (TGF) α in both HCC cells and human squamous cell carcinoma cells undergoing apoptosis [6,7]. ACR induces the expression of interferon receptor, and also the expression and activity of signal transducer and activator of transcription (STAT) 1 during suppression of cell growth and induction of HCC cell apoptosis [8]. However, it is unclear whether these phenomena are dependent on the restoration of RARα/RXRα.

Transglutaminase 2 (TG2) is a member of a family of crosslinking enzymes that catalyze a post-translational modification of proteins by a calcium-dependent crosslinking reaction that forms N-ε (γ-glutamyl) lysine bonds [9-12]. TG2 has been implicated in apoptosis, although the mechanisms are unknown. Recently, we demonstrated that TG2 induces caspase-independent apoptosis in ethanol-treated hepatocytes by crosslinking and inactivation of the general transcription factor, Sp1, thereby reducing Sp1-dependent expression of growth factor receptors [9,13]. However, whether TG2-induced apoptosis pathway is involved in apoptotic signaling in other cell types or is induced by stimulation with anticancer reagents remains unclear.

Piedrafita *et al.* [14] reported that retinoid-induced apoptosis of T cells accompanies degradation of Sp1 downstream of the caspase pathway. Shao *et al.* [15] found that ACR inhibits the growth of HCC cells by reducing the expression of an Sp1-transactiviable gene, fibroblast growth factor receptor 3 (FGFR3) [16].

These reports suggest that Sp1 and/or its regulating genes are important in ACR-induced apoptosis pathway in HCC cells. We have therefore tested the hypothesis that ACR can restore the expression of TG2 by preventing phospho-inactivation of RXRα, and downregulate the expression of growth factor receptors by inactivating Sp1 due to both caspase-dependent degradation and TG2-dependent crosslinking. We have used HCC cells in culture and *in vivo* models of both transplantation of HCC into nude mice and *N*-diethylnitrosamine (DEN)-induced rat hepatocarcinogenesis.

Methods

Materials

ACR (NIK-333) was supplied from Kowa Company, Ltd. (Tokyo, Japan). Anti-TG2 monoclonal antibody (TGase II, Ab-1) was purchased from NeoMarkers (Fremont, CA). Anti-TG2 polyclonal antibody was produced as previously described [13]. Mouse anti-Sp1 (IC6), rabbit anti-Sp1 (PEP2), anti-EGFR, anti-c-Met, anti-FGFR1 antibodies were bought from Santa Cruz Biotechnology (Santa Cruz, CA).

Mouse anti-GAPDH antibody was from Millipore (Billerica, MA). Anti-Bcl-X_L and anti-cleaved caspase 3 antibodies were from Cell Signaling Technology (Danvers, MA). Horseradish peroxidase (HRP)-conjugated goat anti-rabbit or mouse IgG was from Jackson ImmunoResearch Laboratories (West Grove, PA). Viable cells were measured using a cell counting kit-8 (Dojindo; Tokyo, Japan). 5-(biotinamido) pentylamine, a biotinylated primary amine substrate for TG2 was provided by Pierce Biotechnology (Rockford, IL). A caspase-3 specific inhibitor, zDEVD-fmk, and Hoechst 33258 came from Calbiochem-Novabiochem (La Jolla, CA). Anti-crosslinked Sp1 (CLSp1) antibody was made in rabbits, and purified as previously described [13].

Cells and plasmids

A HCC cell line, JHH-7 cells kindly supplied by Dr. Matsuura (Jikei University School of Medicine, Tokyo, Japan) [17] were maintained in ASF104 medium (Ajinomoto, Tokyo, Japan). HC cells, a normal human hepatocyte cell line purchased from Cell Systems (Kirkland, WA), were cultured in CS-C complete medium (Kirkland, WA) [4]. HuH-7, HepG2, and HelaS3 cells were maintained in RPMI 1640 medium containing 10% FBS. The expression vector for human Sp1 (*Sp1-pCIneo*) was constructed as previously described [18]. The TG2, Sp1, and EGFR siRNA-expressing lentiviral vectors were constructed in the pSIH-H1 shRNA vector (SBI System Biosciences, CA). A GC3-Luc vector, containing 3 sequential repeats of GC box motifs derived from the *EGFR* promoter [19] and its TATA box sequence upstream of the luciferase cDNA, was generated by inserting a synthesized oligodeoxynucleotide cassette into the pGL3 vector (Promega Corp., WI).

Transient transfection

Transfections and assays of luciferase activity were performed with a combination of UNIFECTOR lipofection reagent (B-Bridge International, Inc.; Mountain View, CA) and luciferase reporter genes (firefly- and *Renilla*-Luc) as previously described [20], with further details being provided in the Additional file 1.

TG2 knockdown

Knockdown of TG2 was performed by transfection of anti-sense (AS) or siRNA to TG2 in JHH-7 cells, suppressing the expression of TG2 protein ~50% and ~70%, respectively (Additional file 2 Figure S1)

Preparation of whole lysates and nuclear extracts

Whole lysates were prepared in Hepes buffer containing 10 mM CHAPS and protease inhibitors. Nuclear extracts were prepared as previously described [20].

Western blotting

Western blotting was carried out as previously described [20], using combinations of 1 μg/ml each of anti-Sp1, anti-CLSp1, or anti-TG2 antibody and HRP-conjugated goat anti-rabbit/mouse IgG (1:1,000 dilution). Reactants were detected with Enhanced Chemiluminescence reagents (GE Healthcare, Buckinghamshire, UK).

Reverse transcriptase-polymerase chain reaction (RT-PCR)

RT-PCR was done as before [18], using sets of specific primers summarized in Additional file 3 Table S1.

Staining of cells

Cells grown on cover slips were fixed with 10% formalin in culture medium. They were permeabilized with 0.3% Triton X-100 in TBS (pH 7.4), and stained with the antibodies given in each figure legend. Apoptosis was detected by the terminal deoxynucleotidyl transferase-mediated dUTP nick end-labeling (TUNEL) method with the *In Situ* Cell Death Detection Kit (Roche Diagnostics GmbH; Mannheim, Germany). Digital images of cells were obtained by confocal microscope (Carl Zeiss, Inc. Germany), and digital images recorded.

Animal experiments

One week after JHH-7 cells (2×10^6 /50 μl) had been transplanted into the spleens of nude mice aged 6 weeks (Balb/c Slc-nu/nu, Japan SLC Inc., Shizuoka, Japan), ACR (100 mg/kg/day) or vehicle (soybean oil) was administrated by gavage at 10 μl/g body weight once a day on consecutive days for 3 weeks. The DEN-induced rat hepatocarcinogenesis model was used as previously described [21]. Briefly, 6-week old rats (F344/N SLC; Japan SLC Inc., Shizuoka, Japan) were given drinking water containing 40 ppm DEN (Tokyo Kasei Kogyo Co., Tokyo, Japan) for 15 weeks to produce liver neoplasms. ACR (40 and 80 mg/kg) or vehicle (soybean oil) was administered orally with a stomach tube at 5 μl/g body weight for 14 weeks. Experiments were performed in accordance with protocols approved by the RIKEN Institutional Animal Use and the Care Administrative Advisory Committees.

Immunohistochemistry

Immunohistochemistry were performed as before [13]. Livers were removed, fixed in 10% formalin, and embedded in paraffin wax. Sections were prepared and stained with anti-CLSp1, anti-TG2, anti-cleaved caspase 3, and anti-EGFR polyclonal antibodies. Staining signals were enhanced using an ABC kit (VECTASTAIN) and developed with DAB substrate.

Statistical analysis

Quantitative data are given as means ± SD. Student's *t* test was used to evaluate differences between 2 groups. In comparing data from the vehicle group with those from groups treated with ACR at doses of 25, 50, and 100 mg/kg body weight, the level of serum AFP and the number of AFP-positive mice were analyzed by Dunnett's multiple comparison and Fisher's exact probability test, respectively. A p-value of <0.05 was considered statistically significant.

Results

ACR induces both caspase- and TG2-dependent apoptosis pathways

ACR induced TUNEL-positive apoptosis of JHH-7 cells, but not normal hepatocyte HC cells (Figure 1A, *left panel*). Apoptotic JHH-7 cells were also positive for crosslinked Sp1 (CLSp1; Figure 1A, *right panel*). Strong immunofluorescent spots were obvious in cells undergoing severe apoptosis (Figure 1A, *right panel*, arrows). JHH-7 cells were the most sensitive to ACR of the 3 HCC cell lines (JHH-7, HuH-7, HepG2) and HelaS3 cells (Figure 1B). They showed similar TG2/TUNEL/CLSp1-positive apoptosis following ACR treatment (*data not shown*). Consistent with previous findings with another HCC cell line (HuH-7) [6], ACR treatment of JHH-7 cells, but not HC cells, suppressed phosphorylation of RXRα without affecting the expression of RXRα (Additional file 4 Figure S2A), prevented phospho-inactivation of RXRα, and enhanced the expression of TG2 (Additional file 4 Figure S2B).

Reciprocally in parallel with a dose- and time-dependent decrease in cell number (Figure 1C, *left panels*), both TUNEL (Figure 1C, *middle panels*) and TG2 positivity (Figure 1C, *right panels*) increased in ACR-treated JHH-7 cells undergoing apoptosis. ACR-induced apoptosis was partially blocked by either the inclusion of the caspase inhibitor, z-DEVD (Figure 1D and 1E, *sample 3*) or knocking down by 50% TG2 expression with antisense (AS) TG2 (Figure 1D and 1E, *sample 4*; Additional file 2 Figure S1A), whereas apoptosis was almost completely blocked by their combined inhibition (Figure 1D and 1E, *sample 5*). These results suggest that ACR-induced apoptosis is dependent on both caspase 3 and TG2 activation.

In ACR-treated JHH-7 cells ACR had markedly increased levels of CLSp1 (Figure 1A, *right panel* and Additional file 5 Figure S3A, *lane 4*), whereas levels of the Sp1 monomer decreased (Additional file 5 Figure S3A, *lane 2*), thereby reducing its DNA binding activity (Additional file 5 Figure S3B) and transactivation activity (Additional file 5 Figure S3C), as previously seen in ethanol-induced hepatocyte apoptosis [13]. Impaired Sp1 activity was partially improved either by inhibition of caspase or TG2 knockdown by transfection of ASTG, and almost completely restored by their combination, as also by overexpression of Sp1. These results suggest that

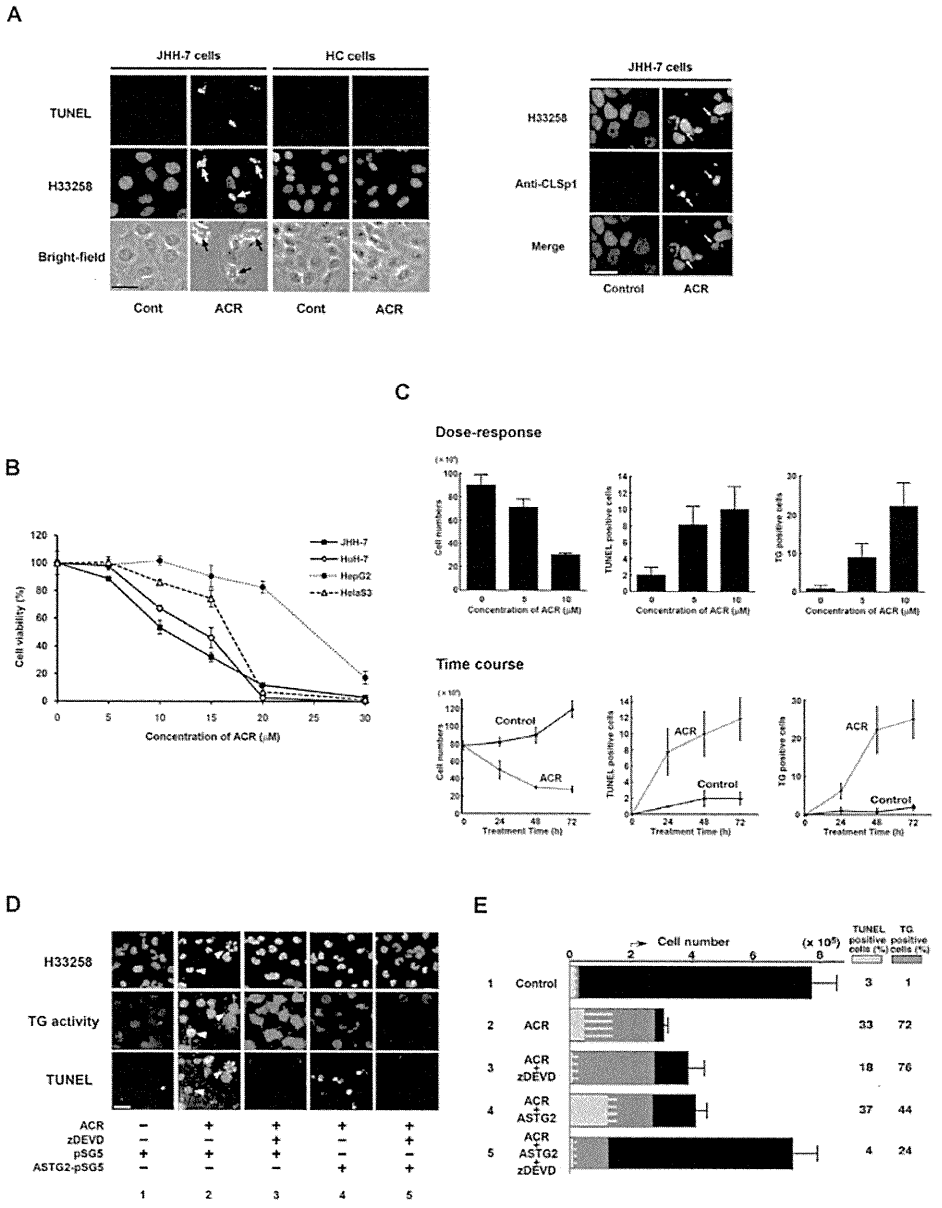

Figure 1 Induction of caspase 3 and TG2- dependent apoptosis by ACR in JHH-7 cell cultures. *A*, JHH-7 and HC cells were seeded in 35 mm dishes containing glass coverslips at 2 × 10^5/dish, and treated with 10 μM ACR or vehicle (0.1% ethanol) for 24 h. Cells were fixed and stained combination with Hoechst 33258, and TUNEL (*left panels*) or anti-CLSp1 antibody (*right panel*). Scale bar, 50 μm. *B*, JHH-7, HuH-7, HepG2 and HelaS3 were seeded at 1 × 10^4 cells/96 well microplates and treated with the indicated concentrations of ACR or vehicle for 24 h. Viable cell counts are plotted as percentages of each control culture treated with vehicle. *C*, JHH-7 cells were seeded as before and treated either with the indicated concentrations of ACR for 48 h, or with 10 μM ACR for the indicated times. Cells were fixed and stained with Hoechst 33258, TUNEL, and anti-TG2 antibody. The numbers of total and apoptotic cells with TUNEL or TG2 positivity in each dish were counted and plotted. *D*, JHH-7 cells were seeded as before and transfected with either pSG5 or anti-sense (AS) TG2-pSG5. The next day cells were treated with either vehicle or 10 μM ACR for 24 h in the presence or absence of 100 μM zDEVD-fmk, with 1 mM 5-(biotinamido)-pentylamine being included during the last 2 h incubation. Cells were fixed and stained with Hoechst 33258 (*upper panels*), TRITC-conjugated streptavidin (*middle panels*), and TUNEL (*bottom panels*). Arrowheads indicate apoptotic cells with chromatin condensation. Scale bar, 50 μm. *E*, JHH-7 cells were treated as in (*C*). The numbers of total and apoptotic cells with TUNEL (green colors) or TG2 (orange colors) positivity in each dish were counted and plotted as bar graphs. Their percentages relative to total cell number are given on the right hand-side of each bar graph. Panels *A-E* show representative results from 3 different experiments with similar results.